PHYSICAL REVIEW LETTERS

Shear Strain in $Nd_{0.5}Ca_{0.5}MnO_3$ at High Pressures

Anthony Arulraj,[1,*] Robert E. Dinnebier,[2] Stefan Carlson,[3] Michael Hanfland,[4] and Sander van Smaalen[1,†]

[1]*Laboratory of Crystallography, University of Bayreuth, D-95440 Bayreuth, Germany*
[2]*Max Planck Institute for Solid State Research, Heisenbergstraße 1, D-70569 Stuttgart, Germany*
[3]*MAX-lab, Lund University, P.O. Box 118, SE-22100 Lund, Sweden*
[4]*European Synchrotron Radiation Facility, BP 220, 38043 Grenoble cedex 9, France*

High-pressure x-ray powder diffraction has been measured on the half doped rare earth manganite $Nd_{0.5}Ca_{0.5}MnO_3$ up to a pressure of 15 GPa. We report the presence of a quantifiable amount of shear distortion of the MnO_6 octahedra in $Nd_{0.5}Ca_{0.5}MnO_3$ at high pressures. The lattice strain of $Nd_{0.5}Ca_{0.5}MnO_3$ is minimal at a crossover pressure of $p^* \sim 7$ GPa, with the same lattice strain above and below this pressure achieved by shear and Jahn-Teller–type distortions, respectively. The increase in shear strain with increasing pressure provides a mechanism for the insulating behavior of manganites at high pressures that has not been considered before.

Colossal magnetoresistance (CMR), the dramatic reduction of electrical resistivity in a magnetic field, and charge ordering (CO) in rare earth manganites $L_{1-x}A_xMnO_3$ (L for rare earths and A for divalent cations) are manifestations of the intricate relation between orbital, spin, charge, and lattice degrees of freedom [1]. The important role of lattice effects in these manganites is now well recognized [2,3]. Any crystal structure can be described by a combination of tilts and Jahn-Teller (JT)– type and shear-type distortions of the MnO_6 octahedra as compared to the hypothetical, high-symmetry cubic perovskite-type crystal structure of these compounds [4–7]. Studies concerned with the relation between physical properties, chemical composition, and crystal structure of CMR manganites have concentrated on variations of the JT distortions and tilts of the MnO_6 octahedra [3], while neglecting shear distortions. Here we report the pressure-dependent crystal structures of half doped manganite $Nd_{0.5}Ca_{0.5}MnO_3$. We have found that the JT distortion decreases and shear distortion increases on increasing pressure. A crossover pressure $p^* \sim 7$ GPa is identified, at which the lattice distortion is at a minimum. Previous high-pressure studies on different manganites have also found crossover pressures p^*, and a variation of the JT distortion with pressure was noticed [8,9]. Here we propose that variations of shear-type distortions of MnO_6 octahedra are of equal importance as variations of JT-type distortions in determining the magnetic and electronic interactions in these systems.

Polycrystalline $Nd_{0.5}Ca_{0.5}MnO_3$ was synthesized by conventional ceramic methods. X-ray powder diffraction showed a single phase with lattice parameters and bond distances as reported in the literature [4]. High-pressure angle-dispersive x-ray powder diffraction was measured at selected pressures up to 14.62 GPa at beamline ID9 of ESRF (Grenoble, France), employing a membrane driven diamond anvil cell with nitrogen as the pressure transmitting medium. The pressure was determined by the ruby

luminescence method, and it was measured before and after recording a diffraction image. Monochromatic x rays [$\lambda = 0.415\,94(2)$ Å] and a Marresearch MAR345 image plate system detector were used. An exposure time of 10 s was selected for each image. Data reduction was performed with the computer program FIT2D [10], resulting in diagrams of corrected intensity versus scattering angle 2θ for each pressure. Each data set could be indexed with an orthorhombic lattice with space group $Pnma$. Accurate lattice parameters and atomic coordinates were obtained by Rietveld refinements employing the program General Structural Analysis System (GSAS) [11].

Lattice parameters decrease smoothly up to the maximum measured pressure of $p = 14.62$ GPa [Figs. 1(a) and 1(b)]. For pressures above 7 GPa the lattice is pseudotetragonal, but the structure refinements give a good fit to the diffraction data only in $Pnma$, and the structure remains orthorhombic in the entire pressure range. A crossover pressure of $p^* \sim 7$ GPa is observed at which $a > c$ for $p < p^*$ changes to $a < c$ for $p > p^*$. The $Pnma$ structure can be derived from the cubic perovskite-type structure by small cooperative tilt rotations of the MnO_6 octahedra, then resulting in $a > c$ [6]. A uniform compression of MnO_6 octahedra would not change this relation, leaving variation of the deformations of the octahedra as the only source for the crossover at p^*.

The lattice strain can be characterized by a dimensionless symmetry-weighted distortion index WD, defined as $WD = (F/3) \times \sum |(a_i - a_o)|/a_i$ with $a_o = (a_1 a_2 a_3)^{1/3}$; F depends on the type of tilt, and a_i ($i = 1, 2, 3$) are the appropriately scaled lattice parameters [5]. The pressure dependence of WD of $Nd_{0.5}Ca_{0.5}MnO_3$ exhibits a minimum at p^* [Fig. 1(c)]. This implies two regimes. For $p < p^*$ increasing pressure reduces the distortion, while for $p > p^*$ increasing pressure enhances the distortion.

The distortion of the crystal structure is commonly described by a cooperative JT distortion of the MnO_6
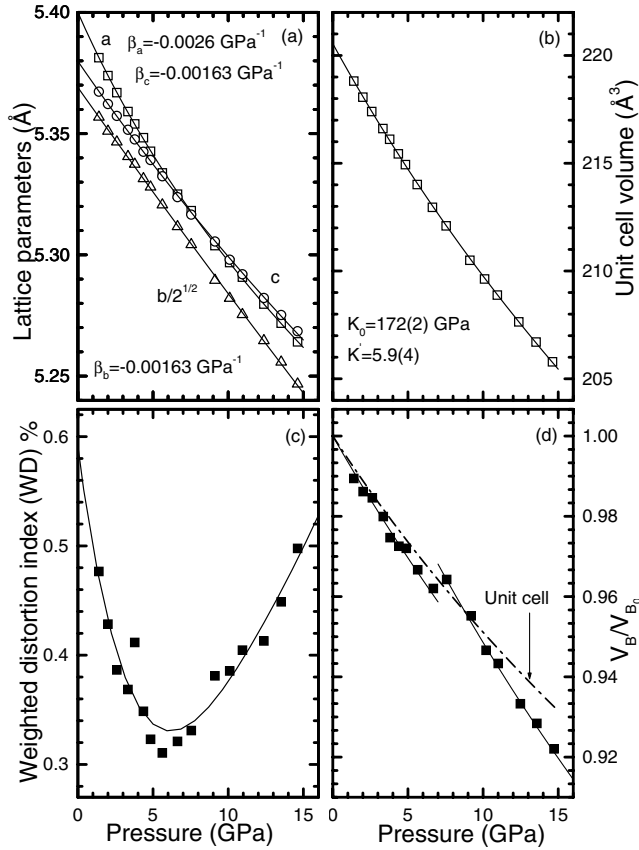
FIG. 1. Pressure dependence of the crystal lattice of Nd$_{0.5}$Ca$_{0.5}$MnO$_3$. (a) Lattice parameters. The solid lines have been obtained by a fit of a Birch-Murnaghan equation of state (EOS) to the individual lattice parameters; the linear compressibility β along the three symmetry directions are indicated [17]. (b) Volume of the unit cell. The solid line is a fit to the Birch-Murnaghan EOS. (c) The evolution of WD (the solid line is a guide to the eye). (d) Volume of the MnO$_6$ octahedra (V_B) normalized to their zero-pressure value (V_{B_0}). The dash-dotted line represents the volume of the unit cell normalized to the zero-pressure value [obtained from (b)].

FIG. 2. Pressure dependence of the local strain of Nd$_{0.5}$Ca$_{0.5}$MnO$_3$. (a) Mn-O distances in the ac plane. The average of the two distances is also given. The dotted line is a guide to the eye. (b) Mn-O distance along the b axis. The dotted line is a guide to the eye. The inset shows the pressure evolution of the Mn-Mn distance in the ac plane (calculated from Mn-O distances and Mn-O-Mn angles). The solid line is the value calculated from the average Mn-O distance in the ac plane. (c) Diagonal components of the local strain tensor. e_{11} is the compression strain along the b symmetry direction and e_{22} and e_{33} are the compression strains along the directions of Mn-O(2a) and Mn-O(2b), respectively. (d) Shear components of the local strain tensor. e_{23} is the shear strain between Mn-O(2a) and Mn-O(2b). The shear strain elements e_{12} and e_{13} involve Mn-O along b with Mn-O(2a) and Mn-O(2b), respectively. Error bars indicate one standard uncertainty. Data points at $p = 4.36$ and 7.58 GPa were considered outliers and were removed from the plots.

octahedra that is defined by the values of the Mn-O bond lengths [12]. The *Pnma* structure type contains three independent Mn-O bond lengths, that are different from each other in Nd$_{0.5}$Ca$_{0.5}$MnO$_3$, indeed. On increasing pressure, the values of the four equatorial bonds approach each other until they are equal for pressures $p > p^*$ [Figs. 2(a) and 2(b)]. At all pressures the two apical bonds are shorter than the average equatorial bond. These results incorrectly suggest that the structural distortion is larger at low pressures than at $p > p^*$. The reason is that the JT distortion affects bond lengths only [1], while possible crystallographic distortions might also lead to deviations of O-Mn-O bond angles from their ideal values of 90° or 180°.

The structure of a MnO$_6$ octahedra in the *Pnma* structure type is completely characterized by three bond lengths and three bond angles that would be equal to each other in the cubic perovskite structure type. In order to separate the isotropic compression (e.g., as achieved by pressure or by variation of the oxidation state of Mn) from the deformation, a local strain tensor can be defined as [7]

$$e_{ij} = \begin{cases} [d(\text{Mn-O}_i) - \langle \text{Mn-O} \rangle]/\langle \text{Mn-O} \rangle, & i = j, \\ [(\pi/2) - (\text{O}_i\text{-Mn-O}_j)], & i \neq j. \end{cases} \quad (1)$$

where $i = 1$ refers to Mn-O(1) along the b axis, and $i = 2, 3$ refer to the two directions, Mn-O(2a) and Mn-O(2b), in the equatorial plane. It is then immediately obvious from Figs. 2(c) and 2(d) that at low pressures the MnO$_6$ octahedra are deformed by anisotropic compression of bonds [large diagonal components $|e_{ii}|$ of Eq. (1)], while at high pressures ($p > p^*$) the octahedra are deformed by shear (large off-diagonal components e_{ij}). It is thus found

that a single state of lattice distortion [single value of WD, Fig. 1(c)] in $Nd_{0.5}Ca_{0.5}MnO_3$ is achieved alternatively by a compressive strain of MnO_6 octahedra (low pressures) or by a shear strain (high pressures).

WD of a distorted perovskite structure may be considered as a sum of components coming from the distortion of the octahedra and their cooperative tilt rotations. The compressibility along different symmetry directions of $Nd_{0.5}Ca_{0.5}MnO_3$ indicates that the lattice distortion is not due to variation of tilts of the MnO_6 octahedra while the pressure evolution of WD above and below p^* can be associated with the shear and JT types of distortions of the MnO_6 octahedra, respectively. The octahedral distortion can be expressed as a dimensionless scalar quantity σ_B, defined as

$$\sigma_B = \sqrt{\sigma^2_{d(Mn\text{-}O)}/\langle Mn\text{-}O\rangle^2} + \sqrt{\sigma^2_\eta/\langle\eta\rangle^2},$$

where

$$\sigma^2_{d(Mn\text{-}O)}/\langle Mn\text{-}O\rangle^2 = (1/6)\sum_{i=1}^{6}[d(Mn\text{-}O_i)/\langle Mn\text{-}O\rangle]^2 - 1$$

represents the JT type distortion, and

$$\sigma^2_\eta/\langle\eta\rangle^2 = (1/4)\sum_{i=1}^{4}(\eta_i/\langle\eta\rangle)^2 - 1$$

represents distortion by shear; $\eta_i = h_i/[(\sqrt{2/3})s_i]$ and is equal to 1 for a regular undistorted octahedron; h_i are the face to face heights of opposite triangular faces of the distorted octahedra, and s_i are the average edge lengths of the triangular faces. The similarities of the pressure dependencies of σ_B and WD [compare Figs. 1(c) and 3(a)] are a clear indication that the pressure-induced lattice distortion in $Nd_{0.5}Ca_{0.5}MnO_3$ is primarily due to the distortions of the MnO_6 octahedra, while the variations of the tilts are less significant. Indeed, the Mn-O-Mn bond angles in the ac plane and along the b direction remain unchanged (within experimental uncertainty) at 153.9 ± 0.3 and 162.2 ± 0.3, respectively.

A comparison of the pressure evolution of the lattice strain in other manganites [8,9] is made through a comparison of their V_A/V_B values [Fig. 3(b)]. An ideal undistorted perovskite structure would have $V_A/V_B = 5$. The tilting of the MnO_6 octahedra in manganites results in a lower value of V_A/V_B in them. Distortions of the A-site and B-site polyhedra also affect this ratio. In $Nd_{0.5}Ca_{0.5}MnO_3$ a decrease in JT distortion of the MnO_6 octahedra for $p < p^*$ is associated with a decrease in distortion of the A-site polyhedra. An approximate measure of this distortion is the difference between the Mn-Mn distance obtained from the actual and the mean Mn-O distances in the ac plane [see inset of Fig. 2(b)]. The application of pressure increases V_A/V_B of $Nd_{0.5}Ca_{0.5}MnO_3$ due to a decrease in the JT-type distortion of the MnO_6 octahedra for $p < p^*$. The shear
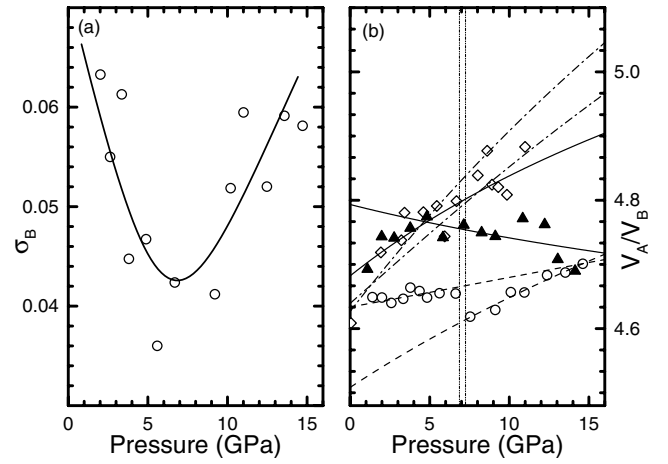
FIG. 3. Pressure dependence of strain in manganites. (a) σ_B of $Nd_{0.5}Ca_{0.5}MnO_3$ (see text). (b) Ratio of the polyhedral volumes V_A/V_B of $Nd_{0.5}Ca_{0.5}MnO_3$ (open circle and dashed line), $LaMnO_3$ (open diamonds and dash-dotted line, from Ref. [9]), $La_{0.75}Ca_{0.25}MnO_3$ (solid triangles and solid line, from Ref. [8]). V_A and V_B are the polyhedral volumes of the A-site and B-site cations, respectively. V_B for $Nd_{0.5}Ca_{0.5}MnO_3$ was calculated from the atomic coordinates of the oxygen atoms and the lattice parameters, while that for $La_{0.75}Ca_{0.25}MnO_3$ and $LaMnO_3$ was calculated from the average Mn-O distances and are likely to be slightly underestimated. The lines are obtained from the EOS fits of the unit cell volume and V_B data, respectively.

deformation of the MnO_6 octahedra at $p > p^*$ leads to a higher compressibility of V_B/V_{B_0} than of V_C/V_{C_0} at these pressures (V_{B_0} and V_{C_0} being the zero-pressure values of the MnO_6 octahedral volume and the unit cell volume, respectively) [Fig. 1(d)]. The pressure dependence of V_A/V_B at $p > p^*$ is thus accounted for by the shear strain in this compound. The pressure evolution of the lattice parameters of $LaMnO_3$ is characterized by a crossover pressure $p = p^* \sim 7$ GPa across which $a > c$ changes to $a < c$ [9]. The pressure evolution of the crystal structure of $LaMnO_3$ is similar to that of $Nd_{0.5}Ca_{0.5}MnO_3$. An increase of the shear strain of the MnO_6 octahedra for $p > p^*$ would be consistent with the observed pressure dependence of V_A/V_B in this compound. So, contrary to the proposed continuous suppression of the distortion [9], it is likely that, for pressures increasing above p^*, shear strain develops in $LaMnO_3$. V_A/V_B of $La_{0.75}Ca_{0.25}MnO_3$ decreases with increasing pressure for $p > p^*$ that is in contrast to the behavior observed in the other two manganites. The crystal structure of $La_{0.75}Ca_{0.25}MnO_3$ is characterized by $a < c$ that implies the presence of strain in MnO_6 following the arguments given in the previous paragraphs. At $p = p^* \sim 7$ GPa an onset of cooperative JT distortion was reported in this compound, wherein equal equatorial Mn-O bonds for $p < p^*$, split into long and short bonds for $p > p^*$ [8], which together with the condition of $a < c$ is the

reason for the decrease in V_A/V_B with increasing pressure [Fig. 3(b)].

Shear strain of the MnO_6 octahedra would necessarily lead to a decrease in the orbital overlap between Mn:e_g orbitals and O:p orbitals and hence provide a mechanism for the localization of the conduction electrons in manganites. Ambient temperature electrical resistance (R) has been shown to decrease with increasing pressure in the manganites $LaMnO_3$ and $La_{0.75}Ca_{0.25}MnO_3$ [8,9]. The reported data for $LaMnO_3$ also shows an increase in the $\partial R/\partial P$ value from a more negative to a less negative value at $p = p^*$ [9] that indicates the onset of an electron localization mechanism.

Subtle structural changes are known to cause substantial changes in the exchange couplings in solids [13,14]. Shear distortion observed in $Nd_{0.5}Ca_{0.5}MnO_3$ at high pressures would always lead to more insulating behavior and could affect the delicate balance between the competing magnetic interactions involving e_g and t_{2g} orbitals of Mn, and p orbitals of O atoms that are known to be important for the physical properties in manganites [1,3]. Recently, pressure activated insulating behavior found by high-pressure and low-temperature transport measurements was reported in the $Pr_{0.7}Ca_{0.3}MnO_3$ manganite [15,16]. Owing to similar mean ionic radii of the A-site cations ($\langle r_A \rangle$) of the manganites $Nd_{0.5}Ca_{0.5}MnO_3$ and $Pr_{0.7}Ca_{0.3}MnO_3$, similar strain effects can be expected in these manganites, and, indeed, the shear strain of the MnO_6 octahedra could be a plausible cause of the pressure activated insulating behavior in $Pr_{0.7}Ca_{0.3}MnO_3$. Much work needs to be done to understand and establish the role of shear distortions of MnO_6 octahedra on physical properties of manganites.

In conclusion, we have found a quantifiable amount of shear distortion in $Nd_{0.5}Ca_{0.5}MnO_3$ at high pressures. Our study shows that variation of pressure affects its crystal structure by decreasing the JT-type distortions ($p < p^*$) and by increasing the shear distortion ($p > p^*$) of the MnO_6 octahedra, while their tilts are not significantly affected. Previous high-pressure studies of manganites considered only the distortions involving the Mn-O bonds. We show that the shear distortion may be present in other manganites as well. While the shear distortion is likely to provide a mechanism for insulating behavior and have consequences on the magnetic interactions in manganites, its precise role in determining the physical properties of manganites is yet to be established.

———————

*Electronic address: anthony.arulraj@uni-bayreuth.de
†Electronic address: smash@uni-bayreuth.de

[1] E. Dagotto, *Nanoscale Phase Separation and Colossal Magnetoresistance: The Physics of Manganites and Related Compounds*, Springer Series in Solid State Sciences Vol. 136 (Springer, New York, 2003).

[2] A. J. Millis, Nature (London) **392**, 147 (1998).

[3] J. B. Goodenough, Rep. Prog. Phys. **67**, 1915 (2004).

[4] P. M. Woodward, T. Vogt, D. E. Cox, A. Arulraj, C. N. R. Rao, P. Karen, and A. K. Cheetham, Chem. Mater. **10**, 3652 (1998).

[5] H. D. Megaw, *Crystal Structures: A Working Approach* (W. B. Saunders Company, Philadelphia, PA, 1973).

[6] M. ÓKeeffe and B. G. Hyde, Acta Crystallogr. Sect. B **33**, 3802 (1977).

[7] Y. Zhao, D. J. Weidner, J. B. Parise, and D. E. Cox, Phys. Earth Planet. Inter. **76**, 1 (1993).

[8] C. Meneghini, D. Levy, S. Mobilio, M. Ortolani, M. Nuñez-Reguero, A. Kumar, and D. D. Sarma, Phys. Rev. B **65**, 012111 (2002).

[9] I. Loa, P. Adler, A. Grzechnik, K. Syassen, U. Schwarz, M. Hanfland, G. K. Rozenberg, P. Gorodetsky, and M. P. Pasternak, Phys. Rev. Lett. **87**, 125501 (2001).

[10] A. P. Hammersley, S. O. Svensson, M. Hansfland, A. N. Fitch, and D. Hausermann, High Press. Res. **14**, 235 (1996).

[11] A. C. Larson and R. B. V. Dreele, "*GSAS: General Structural Analysis System*," LANSCE, Los Alamos National Laboratory, 1994.

[12] P. G. Radaelli, G. Iannone, M. Marezio, H. Y. Hwang, S.-W. Cheong, J. D. Jorgensen, and D. N. Argyriou, Phys. Rev. B **56**, 8265 (1997).

[13] M. A. Korotin, I. S. Elfimov, V. I. Anisimov, M. Troyer, and D. I. Khomskii, Phys. Rev. Lett. **83**, 1387 (1999).

[14] Z. Fang, I. V. Solovyev, and K. Terakura, Phys. Rev. Lett. **84**, 3169 (2000).

[15] C. Congwu and T. A. Tyson, Appl. Phys. Lett. **83**, 2856 (2003).

[16] C. Cui and T. A. Tyson, Phys. Rev. B **70**, 094409 (2004).

[17] R. J. Angel, in *High-Temperature and High-Pressure Crystal Chemistry*, edited by R. M. Hazen and R. T. Downs, Review in Mineralogy and Geochemistry Vol. 41 (Mineralogical Society of America, Washington, DC, 2000), Chap. 2, p. 35.